Impact of binder jetting process parameters on sand mould friability

Jonathan Kabadjundi Kabasele[1*], *Kasongo* Didier Nyembwe[2], and *Mashinini* Madindwa[1]

[1]University of Johannesburg, Engineering Metallurgy, Johannesburg, South Africa
[2]Cape Peninsula University of Technology, Mechanical and Mechatronic Engineering, Bellevue, South Africa

Abstract. The growing application of the binder jetting process for the manufacturing of sand moulds, beyond prototyping, has highlighted the need to understand the effects of process parameters on mould properties. Friability is a crucial foundry property of moulds, related to the resistance of mould erosion during the pouring of liquid metal. In this study, test samples were printed using the Voxeljet VX1000 system and evaluated for friability, with results ranging between 11% and 44%. Artificial Neural Network (ANN) modelling and sensitivity analysis were employed to identify key process parameters affecting friability. AFS (American Foundry Society) grain size emerged as the dominant factor, accounting for 80% of the total impact. Coarser grains significantly improved mould durability by enhancing particle packing and bonding strength. Drop mass (resin concentration) ranked second with a 12% impact, while printhead speed followed closely at 11%. DX (print resolution) exhibited the lowest influence at 6%, indicating that while the distance between drops of binder remains essential for structural integrity, it is not the primary driver of friability. This study is in line with South Africa's strategy for the implementation of additive manufacturing in the foundry industry.

1 Introduction

Rapid sand casting (RSC) is a method of mould manufacturing used in sand casting, which differs from traditional moulding by employing the binder jetting process. This process introduces printing parameters and constructs parts layer by layer without compaction, impacting moulding properties. RSC is being utilized in industries such as automotive manufacturing for aluminium casting prototypes to evaluate intricate designs and ensure defect-free final products efficiently. Studies indicate that castings produced with RSC have properties that are comparable to, or better than, those created using conventional moulding methods [1, 2].

* Corresponding author: kabasele.jonathan@yahoo.fr

1.1 Advantages of sand binder jetting

Binder jetting technology is gaining traction globally, especially in the foundry sector, due to its advanced manufacturing capabilities that surpass traditional moulding techniques. Complex applications, such as the casting of impellers, benefit significantly from this innovative process. Sama et al. [1] project involved creating a 3D printed sand mould, oriented vertically, a challenging task for conventional moulding methods. This approach resulted in defect-free castings (see Figure 1), showcasing the flexibility and precision of 3D sand printing. The ability to design vertically oriented moulds for impellers opens up new possibilities for improving gating systems, aided by casting simulation and CAD software [3].

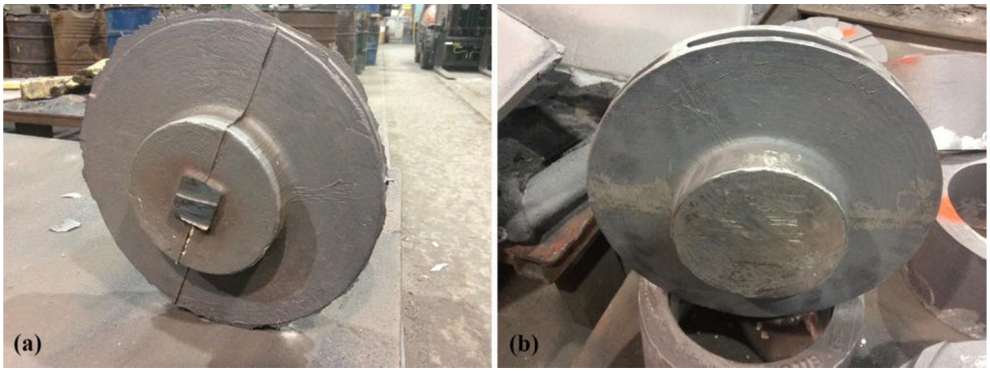

Fig. 1. Casting of a closed vane impeller with a difficult parting line only possible using 3D printed sand mould [1].

Binder jetting technology offers the advantage of merging separate casting moulds into a single mould, including complex feeding passages and a gating arrangement. This process can produce high-quality castings with minimal or no defects. In a case study by Sama et al., eight separate segments of a cast iron bracket were combined in one 3D printed mould with an intricate gating and feeding network. To achieve shrinkage-free casting, each segment required three risers and a shared side riser, as shown in Figure 2. Additionally, four sprues were added to ensure effective metal delivery to areas susceptible to misrun defects [3].

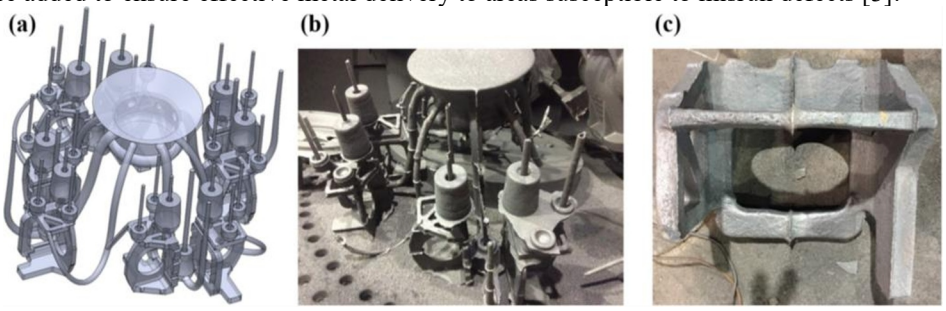

Fig. 2. Complex casting of consolidated eight cast iron bracket produced from a 3D printed sand mould: 2a CAD model of amalgamated cast iron brackets, 2b casting of cast iron brackets, 2c singular bracket with no defects [1].

Several other specialized case studies are published on the benefit of integrating sand binder jetting in the traditional metal casting process. Its capabilities are numerous and noteworthy. It is important to note that the technology differs from conventional moulding and introduces other factors that founders need to consider as the technology transitions from prototyping to a mainstream moulding technique.

1.2 Difference between sand binder jetting and compaction method of moulding

The 3D printing process of binder jetting for sand moulds differs significantly from traditional sand casting. Key differences include porosity between sand grains, mould density, and surface roughness. The lack of compaction and free-fall settling of sand layers can result in poor surface finish. However, for decorative pieces where surface finish or dimensional accuracy is not crucial, binder jetting is preferred. Efforts are being made to introduce a compaction step to improve the sand binder jetting process and prevent binder bleeding [4].

1.3 Parameters of sand binder jetting

The discrepancies observed between 3D printed sand moulds and conventional moulds are primarily attributed to the process parameters of binder jetting printers. The parameters of binder jetting printers are numerous and may slightly vary depending on the printer manufacturer. These parameters include printhead speed, recoater speed, layer thickness, binder concentration, catalyst concentration, sand grain size, binder print orientation and print resolutions. Table 1 highlights the role each parameter plays in the printing of the mould.

Table 1. Parameters of the binder jetting printer [5, 6].

Parameters	Description
Printhead Speed	The speed of the printhead across the printing platform to drop binder droplets.
Recoater Speed	How fast the recoater lays sand on the printing platform
Drop Mass (Binder Concentration)	The amount of biner dropped by the printhead
Print Resolution X	The minimum distance covered by the printhead to drop the binder in the x direction
Print Resolution Y	The minimum distance covered by the printhead to drop the binder in the x direction the Y direction (in the ExOne S-printer Dy is constant at 101.6 μm).
Print Resolution Z	The thicknes of each sand layer deposited (related to granulometry and layer thickness).
Activator or Catalyst Concentration	The concentration of activator or catalyst (e.g., arylsulphonic acid) is used in conjunction with the binder.
Binder Print Orientation	The direction in which the resin is layed against the layer of sand at different angles
Layer thickness	The height of each individual particle layer deposited and bound together during printing; It depends on the type of printer and material.

1.4 Friability of three-dimensionally printed sand mould

Friability is a measure of the surface integrity of the mould or its resistance to erosion during metal casting. High friability test values indicate poor cohesion within the mould, making it unsuitable for casting applications. Conversely, low friability percentages suggest strong bonding and better resistance to erosive forces from liquid metal. Research has shown that fine sand, fillers, hard ramming, and mould paints can help prevent mould erosion [7].

A study by Nyembwe et al investigated the physical properties of sand parts produced using a sand three-dimensional printer. The investigation was comprehensive and studied a range of properties most notably the friability of mould specimens produced by rapid sand casting. The results revealed that the friability of samples produced by binder jetting is between 15 and 35%, an alarming figure for the quality of the final casting [2].

Poor friability and mould erosion cause sand inclusion in castings, leading to surface defects like rough patches and indentations. These inclusions weaken the casting's structural integrity and reduce its mechanical properties, such as strength and ductility. Sand particles trapped in the metal matrix act as stress concentrators, creating points of weakness that increase the risk of premature failure, cracking, or fractures under load, especially in high-stress environments [8].

Sand inclusions can significantly lower a casting's fatigue resistance, which is especially problematic in sectors like automotive and aerospace where components endure repeated loading cycles. Beyond these structural drawbacks, inclusions can disrupt machining by forming localized hard spots that accelerate tool wear, thereby driving up operational expenses. As a result, castings with substantial inclusions frequently fall short of quality specifications, leading to increased rejection rates, rework, and overall production costs [3]. The lack of compaction in 3D sand printing, combined with the influence of newly introduced process parameters, can lead to variability in mould friability, increasing the likelihood of sand inclusions and resulting in substantial losses for foundries. The additive manufacturing principle in the binder jetting process could be the reason for the relatively low friability of three-dimensionally produced sand moulds. Thus, the optimisation of binder jetting parameters and the identification of key parameters affecting friability are crucial to ensuring that moulds produced by binder jetting are defect-free, thereby supporting the efficient adoption of the technology. The study investigates how this property could be optimised by understanding the direct impact of various binder jetting process parameters. The study uses the Artificial Neural Network (ANN) technique followed by sensitivity analysis to understand the impact of input parameters on the friability of 3D printed sand moulds. Ultimately, this research will contribute to the improvement and competitiveness of the binder jetting process for producing superior castings.

1.5 ANN modelling and sensitivity analysis: friability of 3D sand mould

Neural networks utilize a system of interconnected nodes, organized in layers, to process information. Each connection possesses a weight that is adjusted during training, which allows the network to learn from data. The ability of the network to generalize from training data enables it to make predictions or decisions based on new, unseen inputs. Artificial Neural Networks (ANN) are suitable for modelling 3D sand printing, where numerous parameters are involved, and their correlations may not be straightforwardly linear or polynomial [9].

Key input parameters, identified as having the most significant impact on the output, are termed sensitive parameters. Recognizing their sensitivity is crucial; failing to do so can lead to wasted efforts adjusting less relevant parameters, resulting in inefficient model tuning. By identifying and concentrating on sensitive parameters, uncertainty within the model is significantly reduced, leading to more accurate predictions. Sensitivity analysis is

indispensable for evaluating the influence of input parameters, rendering it a critical tool for model development and optimization [10].

The present study employs the forward difference method to conduct sensitivity analysis. This method approximates the central difference method, commonly used for sensitivity analysis. In the forward difference method, the difference between the original and perturbed output is divided by the perturbation amount. For artificial neural networks (ANN), the first set of predicted values, derived from the original inputs, represents the model's baseline performance. The second set of values, obtained after perturbing the input parameters, provides insight into how small changes in the inputs influence the outputs. This is particularly beneficial in ANN models, as understanding the impact of input parameters on the predicted outputs aids in optimizing model performance and identifying sensitive parameters, ultimately enhancing the model's interpretability and accuracy [10].

Equation (1) describes the forward difference method used to perform the sensitivity analysis.

$$\frac{d}{dx}f(x) \approx \frac{f(x+\Delta x)-f(x)}{\Delta x} \tag{1}$$

Where $\frac{d}{dx}f(x)$ represents the sensitivity analysis or how much the output varies when small increment is made on the input parameter. X is the value of the input and ΔX is the perturbation or small increment on the input value. $f(x+\Delta x)$ is the value of an output obtained after an increment is made on the original input. f(x) is the value of the predicted output when no increment is made on the input parameter.

1.6 Novelty of the study

The study conducted by Bobrowski on the characteristics of 3D-printed (binder jetting) furan moulding and core sands, and that of Nyembwe et al. on the suitability of South African silica sand for 3D sand moulding, both provide valuable comparisons of friability between conventionally produced and 3D-printed sand moulds [2, 11]. Bobrowski's work highlights that 3D-printed furan-bonded sands generally exhibit lower friability values, which can improve handling strength but may also affect the mould's ability to collapse after casting. Nyembwe et al. demonstrated that the grain shape, grain size distribution, and binder content of South African silica sands significantly influence friability, especially when used in additive manufacturing processes.

While friability has been addressed in a limited number of studies, there remains a notable gap in the literature regarding the specific contributions of individual binder jetting parameters, such as AFS grain size, drop mass, printhead speed, and print resolution (DX), to friability outcomes. No published research to date systematically ranks or quantifies the relative importance of these parameters.

This is where the present study contributes a novel approach: by applying artificial neural network (ANN) modelling, it is possible to capture complex, non-linear relationships between printing parameters and friability. ANN methods offer the unique advantage of learning from patterns that are not necessarily linear or even directly correlated with standard mathematical functions. Such modelling opens the way for next-generation simulation software capable of predicting and optimising friability during the design phase, thereby mitigating one of the key challenges in 3D sand mould production.

1.7 Aim of the study

The study aims to rank the impact of key parameters influencing the friability of 3D-printed sand moulds, thereby providing operators and foundry engineers with clear guidance on the critical variables to prioritise for process optimisation. In addition, the findings will serve as a foundation for future research and for the development of targeted applications aimed at optimising a broader range of 3D sand moulding properties.

2 Methodology

The experimental work is broken down into four primary stages (refer to Figure 3):

1. Printing of 3D sand moulds using the Voxeljet VX1000 printer.
2. Testing of 3D sand mould friability following the AFS 2248-11-S standard.
3. ANN modelling to rank the impact of binder jetting parameters.
4. Sensitivity analysis of the binder jetting parameters.

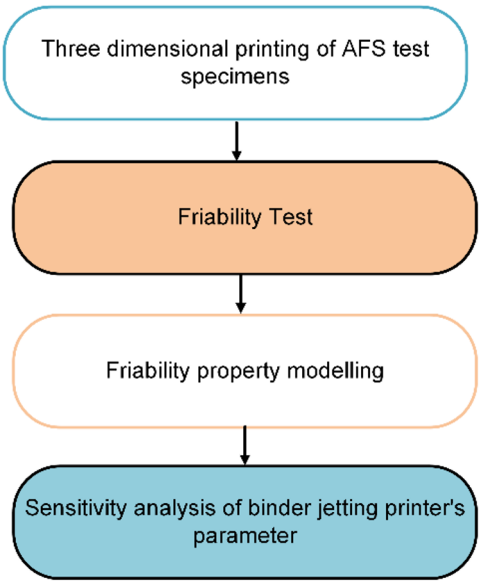

Fig. 3. Experimental procedure.

2.1 Printing of 3D sand moulds using the Voxeljet VX1000 printer

Table 2 details the total number of experiments. Four parameters were considered for the study, and each parameter was varied at 4 levels. The configuration was obtained using an orthogonal array with a L16 design using the Taguchi method. Each experiment configures four input parameters to print a friability sample. The sand samples were coated with an acid catalyst using custom equipment developed at the Vaal University of Technology (see Figure 4). A Voxeljet VX1000 printer was used, with varying parameters including printhead speed (mm/s), drop mass, DX (print resolution), and AFS average grain fineness. The parameters were chosen based on their relevance to the literature, providing a basis for comparison. Additional parameters, including recoater speed, layer thickness, and activator, were excluded following OEM constraints intended to minimise printer failure.

Table 2. VOXELJET VX1000 parameter configuration.

Experiments	DX	Printhead speed	Drop mass	AFS
1	120.00	0.72	1.4997	65.00
2	109.00	0.65	1.6511	64.50
3	102.00	0.61	1.7644	55.00
4	90.00	0.54	1.9996	58.00
5	109.00	0.65	1.6511	55.00
6	120.00	0.72	1.4997	58.00
7	90.00	0.54	1.9996	65.00
8	102.00	0.61	1.7644	64.50
9	102.00	0.61	1.7644	58.00
10	90.00	0.54	1.9996	55.00
11	120.00	0.72	1.4997	64.50
12	109.00	0.65	1.6511	65.00
13	90.00	0.54	1.9996	64.50
14	102.00	0.61	1.7644	65.00
15	109.00	0.65	1.6511	58.00
16	120.00	0.72	1.4997	55.00
17	45.00	0.27	0.5625	55.00

Fig. 4. Binder jetting printer setup: 4a. sand coating machine, 4b. Voxeljet VX 1000 printer, 4c. printed sand test specimen, 4d. coated sand.

2.2 Friability test

In the second step of the experimental procedure, cylindrical test specimens measuring 50 mm in diameter and 50 mm in height are evaluated using a friability tester. Following the AFS 2248-11-S standard, two specimens are placed side by side inside the rotating drums of the tester, which operates at 57 revolutions per minute (RPM) for one minute. As the drum rotates, the samples rub against each other, causing erosion of the outer sand layers. The dislodged sand falls through the drum and is collected on a sheet of paper placed beneath the apparatus. The mass of the eroded sand is then measured using a scale, and the friability percentage is calculated by dividing the eroded mass by the initial mass of the sample. The equipment used is described under Figure 5.

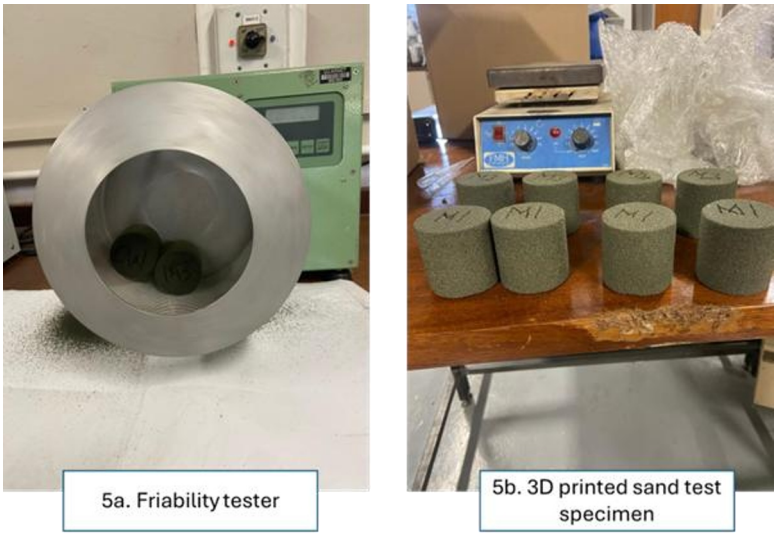

Fig. 5. Friability test setup: 5a Friability tester, 5b 3D printed AFS sand test specimen.

2.3 ANN modelling of friability of 3D printed sand mould test specimens

Figure 6 describes the structure of the friability property model. The model has 4 input parameters, including DX (print resolution), printhead speed, drop mass and AFS average grain fineness, that are configured according to the design of experiment provided in Table 2. The input parameter will serve as the input layer; the hidden layers vary between one and two, and the output layer is the friability of 3D printed sand mould.

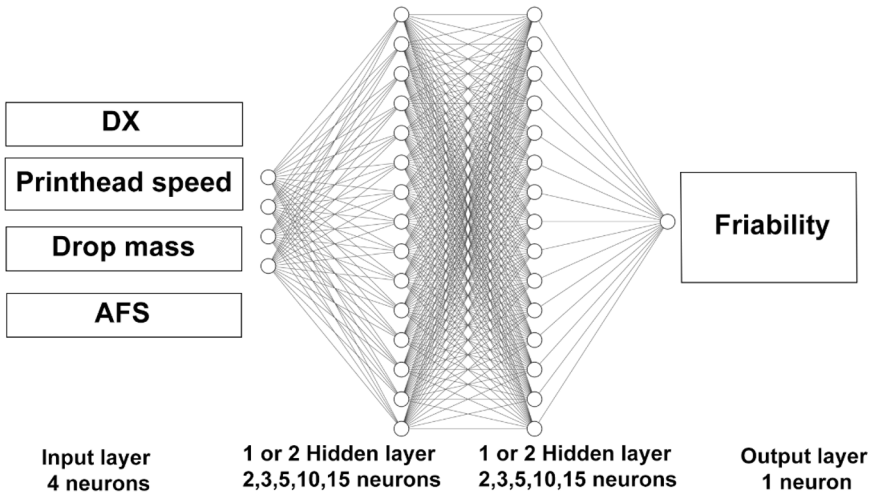

Fig. 6. Structure of friability model.

The parameters of the ANN include three training algorithms: Levenberg-Marquardt (trainlm), Bayesian Regularisation (trainbr), and Scaled Conjugate Gradient (trainscg) [12] [4]. The number of neurons for the hidden layer (layer size) considered was 2, 3, 4, 5, 10, and 15. While the number of hidden layers was set to either 1 or 2. In total, 30 different configurations were tested, and the process was run 10 times. Using these configurations, MATLAB software identifies the optimal model with the highest R-squared coefficient (see Appendix).

2.4 Sensitivity analysis of binder jetting printer's parameter

The forward difference method is implemented in the script (see Appendix) that was run in MATLAB to perform the sensitivity analysis. the script is written according to the structure provided in Figure 7.

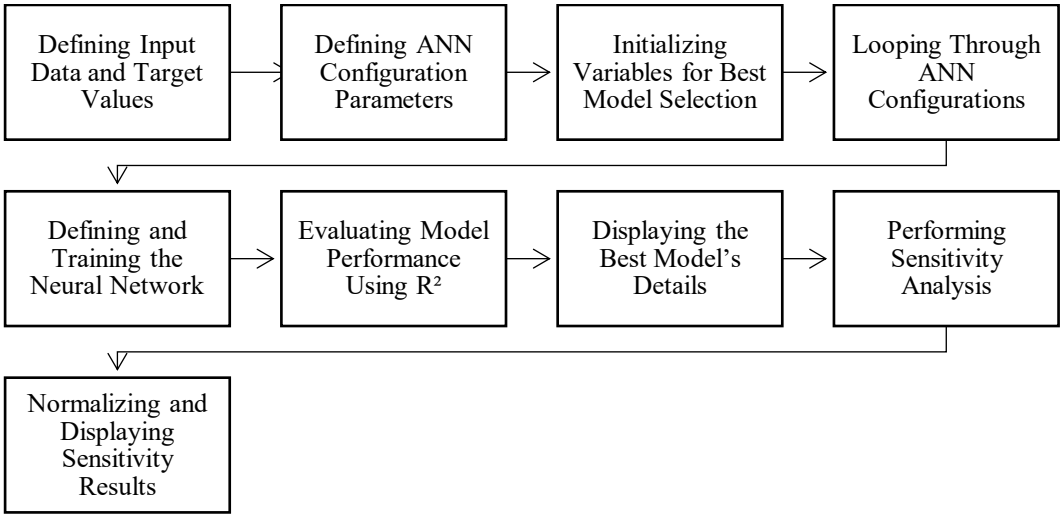

Fig. 7. Breakdown of a sensitivity analysis script.

3 Results and discussion

This section presents the results of the experimental work and discuss the key findings related to the impact of 3D process parameters on the sand friability and the sensitivity analysis.

3.1 Friability test results

The preliminary results are listed in Table 1. The friability results range between 11% and 44%. In general, mould produced with coarser grains (AFS 55) performs better than mould printed with finer grains in terms of friability. The packing density and strength of cohesion is higher compared to finer grains improves the resistance to sand erosion.

Table 3. Friability test results.

AFS	Printhead speed	Drop mass	DX	Friability
55	0.27	0.5625	45	11.49
	0.54	1.9996	90	14.44
	0.61	1.7644	102	17.81
	0.65	1.6511	109	19.01
	0.72	1.4997	120	15.35
58	0.54	1.9996	90	31.11
	0.61	1.7644	102	43.83
	0.65	1.6511	109	43.77
	0.72	1.4997	120	42.15
64.5	0.54	1.9996	90	28.09
	0.61	1.7644	102	40.71
	0.65	1.6511	109	38.24
	0.72	1.4997	120	36.42
65	0.54	1.9996	90	38.26
	0.61	1.7644	102	24.17
	0.65	1.6511	109	28.41
	0.72	1.4997	120	29.05

3.2 Sensitivity analysis results

The most accurate Friability ANN model was achieved with the algorithm Levenberg-Marquardt (trainlm), 10 neurons in the hidden layer, and a single hidden layer. The ANN model demonstrates a high predictive capability, with an R^2 value of 0.9564, indicating a strong correlation between the predicted and actual values. Figure 8 describes the regression values obtained from the ANN model.

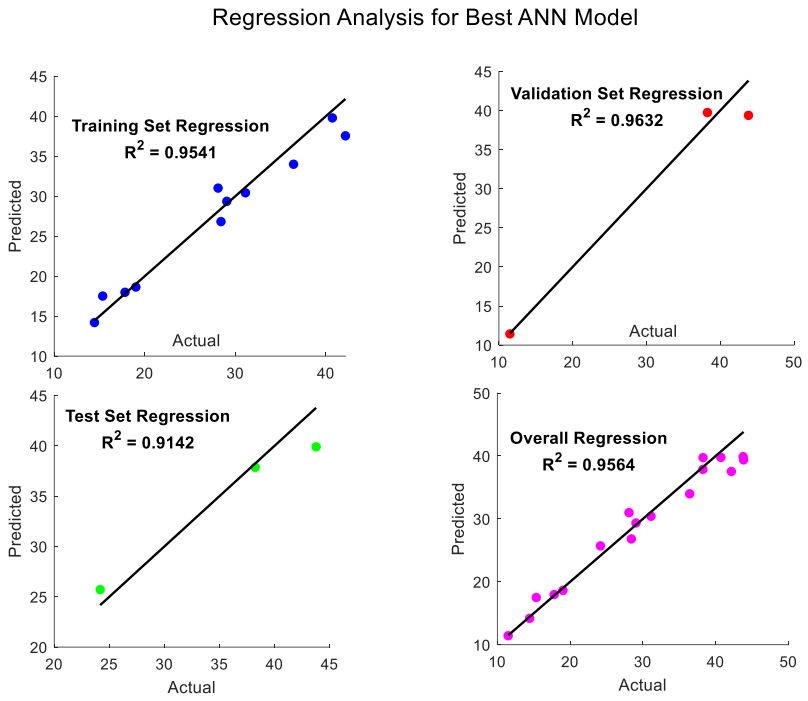

Fig. 8. Friability model (trainlm, 10 neurons, 1 hidden layer) regression results.

Table 4 provides the sensitivity analysis results for each input parameter. DX is input parameter 1, printhead speed drop mass, and AFS are input parameters 2, 3, and 4, respectively. The parameters affecting the friability of 3D sand moulds, in order of impact, are AFS grain fineness, DX (print resolution), printhead speed, and drop mass.

Table 4. Sensitivity analysis report for the friability model.

Parameter	**Normalized Sensitivity**			**Average Sensitivity%**	**Standard deviation**
DX	0.07	0.06	0.06	6.34	0.01
Printhead Speed	0.08	0.04	0.11	7.68	0.03
Drop Mass	0.02	0.04	0.12	5.89	0.04
AFS	0.83	0.86	0.71	80.09	0.07

3.3 Discussion of sensitivity analysis results

Figure 9 describes the percentage of the impact for each parameter on the friability of the mould. Figure 10 shows the normalized sensitivity values for the four input parameters, and error bars represent the variation (standard deviation) in those values across the tests.

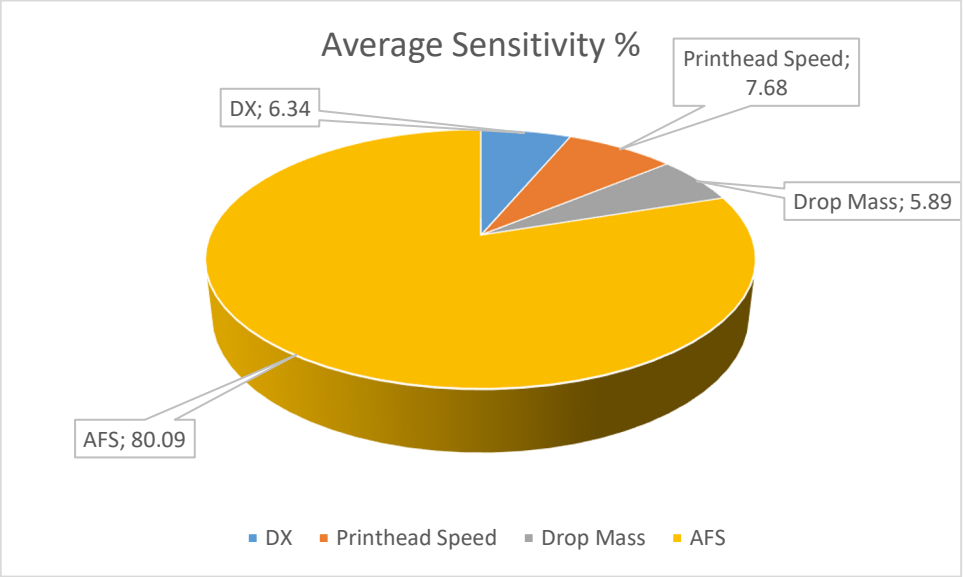

Fig. 9. Average percentage impact on friability of mould specimen.

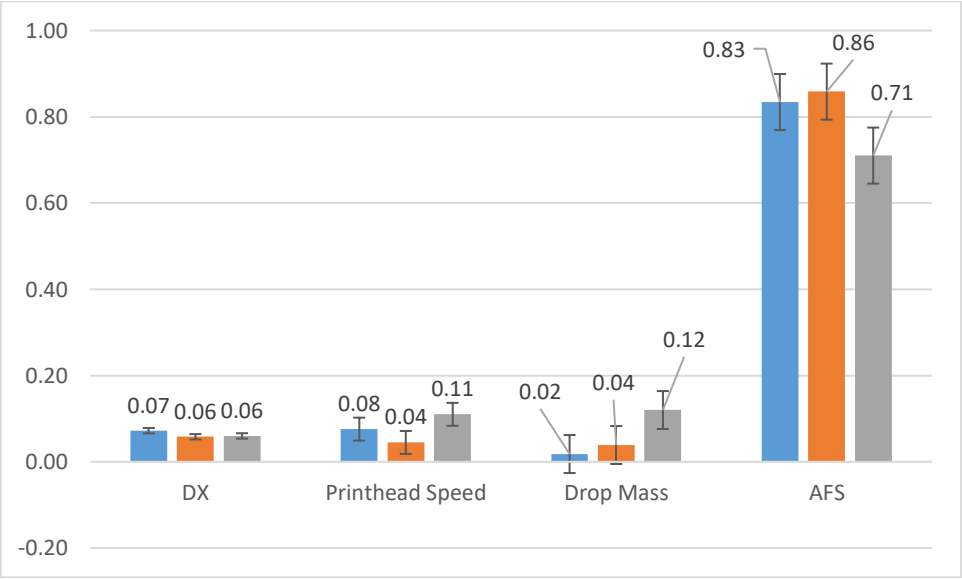

Fig. 10. Normalized sensitivity values for the four binder jetting printers' parameters.

The error bars described in Figure 10 represent the variability in the model's sensitivity estimates across different runs. AFS grain size shows minimal variation, indicating that the model consistently identifies it as the dominant factor influencing friability. In contrast, DX and Drop Mass display greater variability, suggesting that their influence is more dependent on specific process conditions. Printhead Speed shows moderate variation, with its effect generally stable but not as consistent as AFS. Overall, smaller error bars indicate higher confidence in the stability of the sensitivity ranking, while larger error bars reflect parameters whose influence may fluctuate.

According to Figures 9 and 10, AFS grain size is the most influential factor, contributing 80% to the total impact on friability. This highlights the importance of grain size in

determining the mould's resistance to erosion. Coarser grains (represented by lower AFS values) tend to yield lower friability, which is beneficial for producing durable moulds and minimizing sand inclusions in castings. The improved packing density and stronger interparticle bonding provided by coarser grains enhance the structural integrity of the sand mould. Thus, optimizing grain size is crucial for achieving robust mould performance and reducing friability.

Printhead speed ranks second, contributing 7.68% to the overall impact. This parameter controls how binder is deposited onto the sand layer, influencing the uniformity of binder distribution. An optimal printhead speed ensures even binder coverage, improving grain bonding and reducing weak spots in the mould. Poor calibration can negatively affect mould quality, leading to inconsistencies in strength and durability.

DX ranks third, accounting for 6.34% of the impact on friability. Although its standalone effect is limited, DX, which controls the spacing between binder droplets, still contributes to the consistency of binder application and overall bonding quality. Adjusting DX alone is unlikely to improve mould strength significantly.

Drop mass, representing the binder content, has the least influence at 5.89%. While its overall contribution is small, binder content still plays a role in determining sand grain cohesion. Proper binder application enhances the structural integrity of the mould, while excessive binder may reduce permeability, and insufficient binder can lead to weak bonding and fragile moulds.

4 Recommendations

The author acknowledges that conducting a full factorial experiment with as many as 256 runs could potentially yield further insights into the interactions among parameters in sand binder jetting printers. This will be the focus of future work aimed at refining and expanding the scope of the study.

5 Conclusion

Optimising the AFS grain size is crucial for enhancing friability, while drop mass and printhead speed play moderate roles. DX (print resolution) has a smaller impact on mould consistency. This study ranks binder jetting parameters to improve mould friability, supporting South Africa's additive manufacturing strategy in local foundries. The findings serve as a foundational and novel approach to optimising the properties of 3D sand moulds, with potential applications for improving other characteristics of 3D sand moulds. Additionally, this study is instrumental in promoting the additive manufacturing process in South African sand-casting foundries. Future research will investigate other mechanical properties, including strength and toughness.

The author thanks the collaborative program for additive manufacturing (CPAM). Special thanks to the University of Johannesburg and the Vaal University of Technology
Data availability: Data supporting the findings of this study can be made available by the corresponding authors upon reasonable request.

References

1. S. Cecchel and G. Cornacchia, Additive manufacturing for rapid sand casting: mechanical and microstructural investigation of aluminum alloy automotive prototypes, Metals. **14**, 459 (2024). https://doi.org/10.3390/met14040459

2. K. Nyembwe, M. Mashila, P. v. Tonder, D. d. Beer and E. Gonya, Physical properties of sand parts produced using a Voxeljet VX1000 three-dimensional printer, SAJIE. **27**, 136 (2016). https://doi.org/10.7166/27-3-1661
3. S. R. Sama, G. Manogharan and T. Badamo, Case studies on integrating 3d sand-printing technology into the production portfolio of a sand-casting foundry, Inter Metalcast. **14**, 12 (2020). https://doi.org/10.1007/s40962-019-00340-1
4. K. J. Hodder and R. J. Chalaturnyk, Bridging additive manufacturing and sand casting: Utilizing foundry sand, Add. Man. **28**, 649 (2019). https://doi.org/10.1016/j.addma.2019.06.008
5. T. Sivarupan, M. E. Mansori, N. Coniglio and M. Dargusch, Effect of process parameters on flexure strength and gas permeability of 3D printed sand molds, Jour of Man Proc. **54**, 420 (2020). https://doi.org/10.1016/j.jmapro.2020.02.043
6. G. Gao, W. Zhang, Z. Du, Q. Liu, Y. Su and D. Shi, Investigation of selected parameters effect on 3D printed sand mold properties through Taguchi method, Rap Prot Jour. **27**, 627 (2020). https://doi.org/10.1108/RPJ-11-2019-0294
7. P. Beeley, Foundry Technology, (Butterworth-Heinemann, Oxford, 2001).
8. J. Campbell, Complete Casting Handbook: Metal Casting Processes, Metallurgy, Techniques and Design, (Butterworth-Heinemann, USA, 2015).
9. I. Goodfellow, Y. Bengio and A. Courville, Deep Learning, (MIT Press, Cambridge, 2016).
10. D. Yeung, I. Cloete, D. Shi and w. N. Wing, Sensitivity analysis for neural networks, (Springer, New York, 2010).
11. A. Bobrowski, K. Kaczmarska, D. Drożyński, F. Woźniak, M. Dereń, B. Grabowska, S. Żymankowska-Kumon and M. Szucki, 3D Printed (binder jetting) furan molding and core sands—thermal deformation, mechanical and technological properties, Materials. **16**, 3339 (2023). https://doi.org/10.3390/ma16093339
12. E. Uwimana, Y. Zhou and N. Sall, A short-term load demand forecasting: levenberg–marquardt (LM), bayesian regularization (BR), and scaled conjugate gradient (SCG) optimization algorithm analysis, J. Supercomput. **81**, 55 (2025). https://doi.org/10.1007/s11227-024-06513-y

6 Appendix

Table 5 outlines the parametric configurations used for the ANN models.

Table 5. Parametric configurations of ANN models.

Models	algorithm	layer size	number of layers
1	trainlm	2	1
2	trainlm	2	2
3	trainlm	3	1
4	trainlm	3	2
5	trainlm	5	1
6	trainlm	5	2
7	trainlm	10	1
8	trainlm	10	2
9	trainlm	15	1
10	trainlm	15	2
11	trainbr	2	1
12	trainbr	2	2
13	trainbr	3	1
14	trainbr	3	2
15	trainbr	5	1
16	trainbr	5	2
17	trainbr	10	1
18	trainbr	10	2
19	trainbr	15	1
20	trainbr	15	2
21	trainscg	2	1
22	trainscg	2	2
23	trainscg	3	1

24	trainscg	3	2
25	trainscg	5	1
26	trainscg	5	2
27	trainscg	10	1
28	trainscg	10	2
29	trainscg	15	1
30	trainscg	15	2

The script below was used to perform the sensitivity analysis of the tensile strength ANN model in MATLAB.

```
% Define your input data and target values
x = parameters';  % Input data (transpose for MATLAB ANN)
t = friability';  % Target output (transpose for MATLAB ANN)

% Define ranges for ANN configurations
trainFcns = {'trainlm', 'trainbr', 'trainscg'};  % Training algorithms
layerSizes = [2, 3, 5, 10, 15];  % Number of neurons in hidden layer(s)
numLayers = [1, 2];  % Number of hidden layers
numRuns = 10;  % Number of runs per configuration

% Initialize variables to track the best model
bestNet = []; % Store the best trained network
bestR2Overall = -Inf; % Track the highest overall R^2 value
bestTrainFcn = '';
bestLayerSize = 0;
bestNumLayers = 0;
bestTr = []; % Store training record of best model

% Loop through each ANN configuration
for i = 1:length(trainFcns)
    for j = 1:length(layerSizes)
        for k = 1:length(numLayers)
            for run = 1:numRuns
                % Define network architecture
                if numLayers(k) == 1
                    hiddenLayerSize = layerSizes(j);
                else
                    hiddenLayerSize = [layerSizes(j), layerSizes(j)];
```

```
            end

            % Create and configure network
            net = fitnet(hiddenLayerSize, trainFcns{i});
            net.divideParam.trainRatio = 70/100;
            net.divideParam.valRatio = 15/100;
            net.divideParam.testRatio = 15/100;

            % Train network
            [net, tr] = train(net, x, t);

            % Predictions for the entire dataset
            y_pred = net(x);

            % Calculate overall R²
            R2_overall = 1 - sum((t - y_pred).^2) / sum((t - mean(t)).^2);

            % Check if this model is the best so far
            if R2_overall > bestR2Overall
                bestR2Overall = R2_overall;
                bestNet = net;
                bestTrainFcn = trainFcns{i};
                bestLayerSize = layerSizes(j);
                bestNumLayers = numLayers(k);
                bestTr = tr;
            end
        end
    end
  end
end

% Display best model details
disp('Best ANN Model Found:');
disp(['Training Function: ', bestTrainFcn]);
disp(['Layer Size: ', num2str(bestLayerSize)]);
disp(['Number of Layers: ', num2str(bestNumLayers)]);
disp(['Best Overall R² Value: ', num2str(bestR2Overall)]);

% Additional training info
disp(['Total Epochs: ', num2str(bestTr.num_epochs)]);
disp(['Best Performance (MSE): ', num2str(min(bestTr.perf))]);
```

```
if isfield(bestTr, 'vperf')
    disp(['Best Validation Performance (MSE): ', num2str(min(bestTr.vperf))]);
end
if isfield(bestTr, 'mu')
    disp(['Final Mu: ', num2str(bestTr.mu(end))]);
end
if isfield(bestTr, 'gradient')
    disp(['Final Gradient: ', num2str(bestTr.gradient(end))]);
end

% Sensitivity Analysis
[numSamples, numParameters] = size(parameters);
sensitivityResults = zeros(1, numParameters);

for i = 1:numParameters
    % Perturb only the i-th parameter across all experiments
    perturbedParameters = parameters;
    perturbAmount = 0.01 * mean(parameters(:, i));
    perturbedParameters(:, i) = parameters(:, i) + perturbAmount;

    % Predict output using original and perturbed inputs
    originalPrediction = bestNet(parameters');
    perturbedPrediction = bestNet(perturbedParameters');

    % Calculate the average absolute change in output
    sensitivityResults(i) = mean(abs(perturbedPrediction - originalPrediction));
end

% Normalize sensitivity results
normalizedSensitivity = sensitivityResults / sum(sensitivityResults);

% Display the results
disp('Raw Sensitivity Analysis Results:');
for i = 1:numParameters
    fprintf('Input Parameter %d: %f\n', i, sensitivityResults(i));
end

disp('Normalized Sensitivity:');
for i = 1:numParameters
    fprintf('Input Parameter %d: %f\n', i, normalizedSensitivity(i));
end
```

```
% Make predictions for the train, validation, test, and overall sets
trainPred = bestNet(x(:, bestTr.trainInd));
valPred = bestNet(x(:, bestTr.valInd));
testPred = bestNet(x(:, bestTr.testInd));
overallPred = bestNet(x);

% Get actual target values
trainActual = t(bestTr.trainInd);
valActual = t(bestTr.valInd);
testActual = t(bestTr.testInd);
overallActual = t;

% Compute R² values
R2_train = 1 - sum((trainActual - trainPred).^2) / sum((trainActual -
mean(trainActual)).^2);
R2_val = 1 - sum((valActual - valPred).^2) / sum((valActual - mean(valActual)).^2);
R2_test = 1 - sum((testActual - testPred).^2) / sum((testActual - mean(testActual)).^2);
R2_overall = 1 - sum((overallActual - overallPred).^2) / sum((overallActual -
mean(overallActual)).^2);

% Regression Plots
figure;

subplot(2, 2, 1);
scatter(trainActual, trainPred, 'b', 'filled'); hold on;
plot([min(trainActual) max(trainActual)], [min(trainActual) max(trainActual)], 'k',
'LineWidth', 1.5);
xlabel('Actual'); ylabel('Predicted');
title({['Training Set Regression'], ['R^2 = ', num2str(R2_train, '%.4f')]});
hold off;

subplot(2, 2, 2);
scatter(valActual, valPred, 'r', 'filled'); hold on;
plot([min(valActual) max(valActual)], [min(valActual) max(valActual)], 'k', 'LineWidth',
1.5);
xlabel('Actual'); ylabel('Predicted');
title({['Validation Set Regression'], ['R^2 = ', num2str(R2_val, '%.4f')]});
hold off;

subplot(2, 2, 3);
```

```
scatter(testActual, testPred, 'g', 'filled'); hold on;
plot([min(testActual) max(testActual)], [min(testActual) max(testActual)], 'k', 'LineWidth',
1.5);
xlabel('Actual'); ylabel('Predicted');
title({['Test Set Regression'], ['R^2 = ', num2str(R2_test, '%.4f')]});
hold off;

subplot(2, 2, 4);
scatter(overallActual, overallPred, 'm', 'filled'); hold on;
plot([min(overallActual) max(overallActual)], [min(overallActual) max(overallActual)], 'k',
'LineWidth', 1.5);
xlabel('Actual'); ylabel('Predicted');
title({['Overall Regression'], ['R^2 = ', num2str(R2_overall, '%.4f')]});
hold off;

sgtitle('Regression Analysis for Best ANN Model');
```